ULTRASOUND NEWS

August 2026

ScientificScholar®
Knowledge is power
Publisher of Scientific Journals

www.americanjs.com

American Journal of Sonography

Review Article

Emergency Breast Imaging, What Radiologists Need To Know

Abdelmohsen Radwan Hussien[1], Monaliza El-Quadi[2], Rola Shaheen[3], Mohamed Elfar[4], Avice O'Connell[5]

[1]Department of Radiology, SUNY Upstate Medical University, Syracuse, [2]University of Rochester, [3]Department of Radiology, Peterborough Regional Health Center, Peterborough, Ontario, Canada, [4]Department of Surgery, Garnet Health Medical Center, Middletown, [5]Department of Radiology, University of Rochester, Rochester, New York, United States.

***Corresponding author:**
Abdelmohsen Radwan Hussien,

ABSTRACT

Awareness by the general radiologist of the various emergent conditions of the breast would enable a better management and appropriate referral, rather than postponing management till a breast radiologist is available for consultation. Early referrals are essential to prevent deterioration of complications including severe infection and even sepsis. There has been a lack of consensus in the past regarding appropriate management and delays in treatment have resulted in worse outcomes which could have been avoided.

Keywords: Mastitis, Breast abscess, Puerperal mastitis, Inflammatory carcinoma, Ultrasound

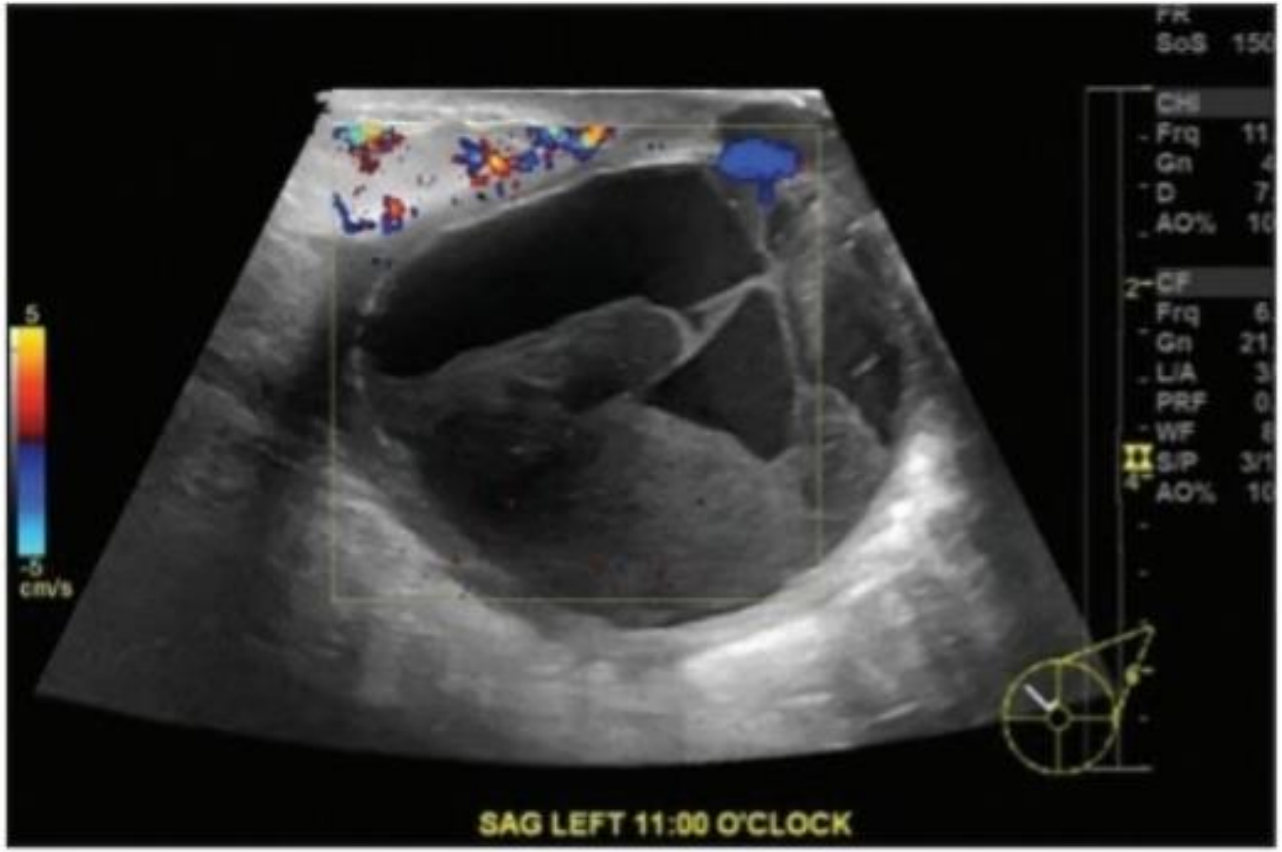

Figure 22: A 59 year old female with breast pain and redness in the region of the surgical bed, status post partial mastectomy. In the region of surgical bed, ultrasound shows a thick walled complex fluid collection at 11-12:00 O'Clock position, with mixed solid and fluid components consistent with infected seroma.

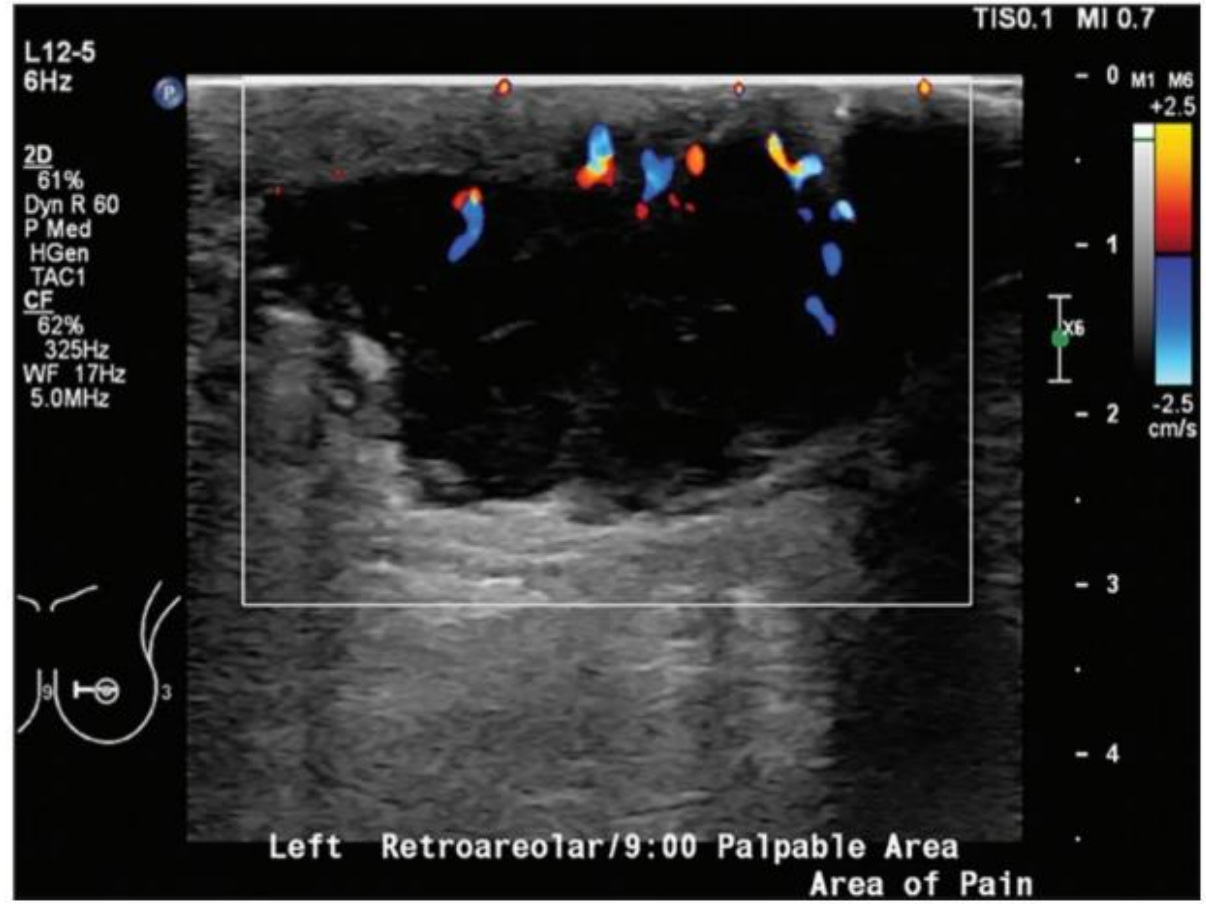

Figure 1: A 37-year-old female with the left breast pain and redness. Ultrasound image shows a complex mixed echogenicity collection with a peripheral vascularity and thick septations consistent with an abscess in the left breast.

CONCLUSION

- Emergency radiologist awareness of common breast presentations in the ED is very important. The main presentations are infection in lactating and nonlactating women including mastitis, cellulitis, or chronic granulomatous mastitis. Evaluation of an abscess and drainage may provide immediate relief
- Inflammatory cancer may mimic infection and differentiation is very important. Follow-up in the breast clinic after a course of antibiotic treatment is the best way to deal with this possibility
- Mondor's disease is an easily missed diagnosis given its rarity. Follow-up in the non-emergency clinic is appropriate
- Biopsy of a mass in a lactating woman may lead to milk fistula. However, if the finding is suspicious, biopsy recommendation should always be made regardless of this possibility. This is usually referred to the breast clinic
- Identification of ruptured breast implants on CT should always be kept in mind
- Patients present with pain or discharge in the ED are quite common. If ultrasound is negative for mass, a follow-up mammogram on non-emergent basis would be reasonable.

ORIGINAL RESEARCH PAPERS

Establishing reference values and evaluating diagnostic utility of scrotal ultrasound for azoospermia subtypes: A cross-sectional study in Guangdong, China

HERAN CAO[1,2#], ZHIXING ZHANG[1,3#], LU HAN[1,4], HUA NIE[1,2], XIAOHUA LIU[1,2], WEIBING QIN[1,2]

ABSTRACT

Background: Male infertility is a significant health issue in East Asia, affecting over 12 million men, primarily due to non-obstructive and obstructive azoospermia. Although scrotal color Doppler ultrasonography is widely used to assess male reproductive health, existing diagnostic standards derived from European populations remain unvalidated for Chinese men. This study aimed to establish population-specific reference values and evaluate the diagnostic utility of ultrasonographic parameters in differentiating azoospermia subtypes.

Methods: We enrolled 424 men aged 20–45 years, including 245 normozoospermic controls, 135 with non-obstructive azoospermia, and 44 with obstructive azoospermia from Guangdong Province, China. All participants underwent scrotal ultrasound following standardized protocols to measure testicular volume, epididymal dimensions, and hemodynamic parameters. Semen analysis and hormonal profiling were also performed.

Results: Results showed that testicular volumes in fertile men from Guangdong Province, China were significantly smaller than European reference values. Testicular volume was inversely correlated with follicle-stimulating hormone and luteinizing hormone levels and positively correlated with sperm count and concentration, but not with those with obstructive azoospermia showed significant dilation of the epididymal caput.

Conclusions: This study provides the first scrotal ultrasound reference standards for men from Guangdong Province, China and suggests that a two-parameter approach based on testicular volume and epididymal caput diameter may aid in non-invasive differentiation of azoospermia subtypes, potentially reducing the need for invasive biopsies.

Key words: Scrotal color Doppler ultrasonography, Non-obstructive azoospermia, Obstructive azoospermia

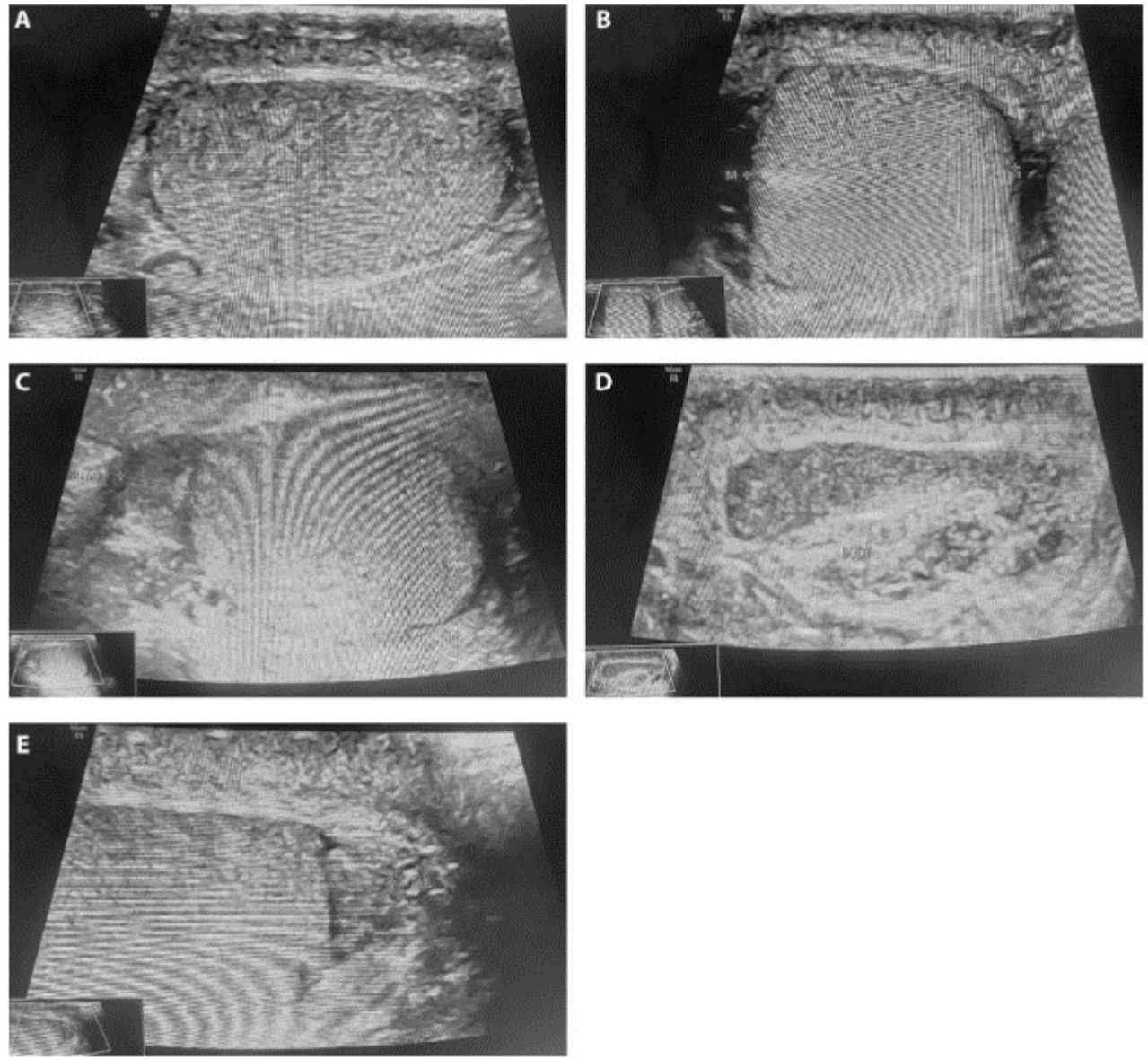

Figure 2. Ultrasonographic visualization and anatomical landmarks of the testis and epididymis. (A) longitudinal diameter (length [L]) in longitudinal scan. (B) anterior-posterior diameter (height [H]) and transverse diameter (width [W]) in transverse scan. (C) Normal epididymal head with triangular shape in a longitudinal scan. (D) Homogeneous epididymal body in a longitudinal scan. (E) Homogeneous epididymal tail in a longitudinal scan.

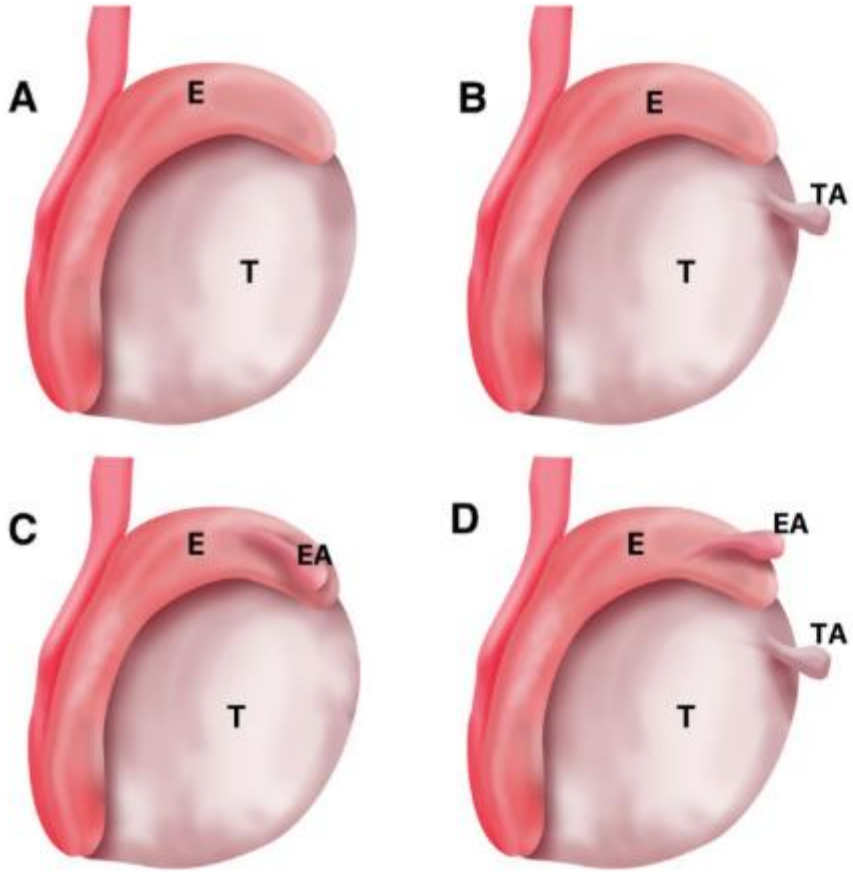

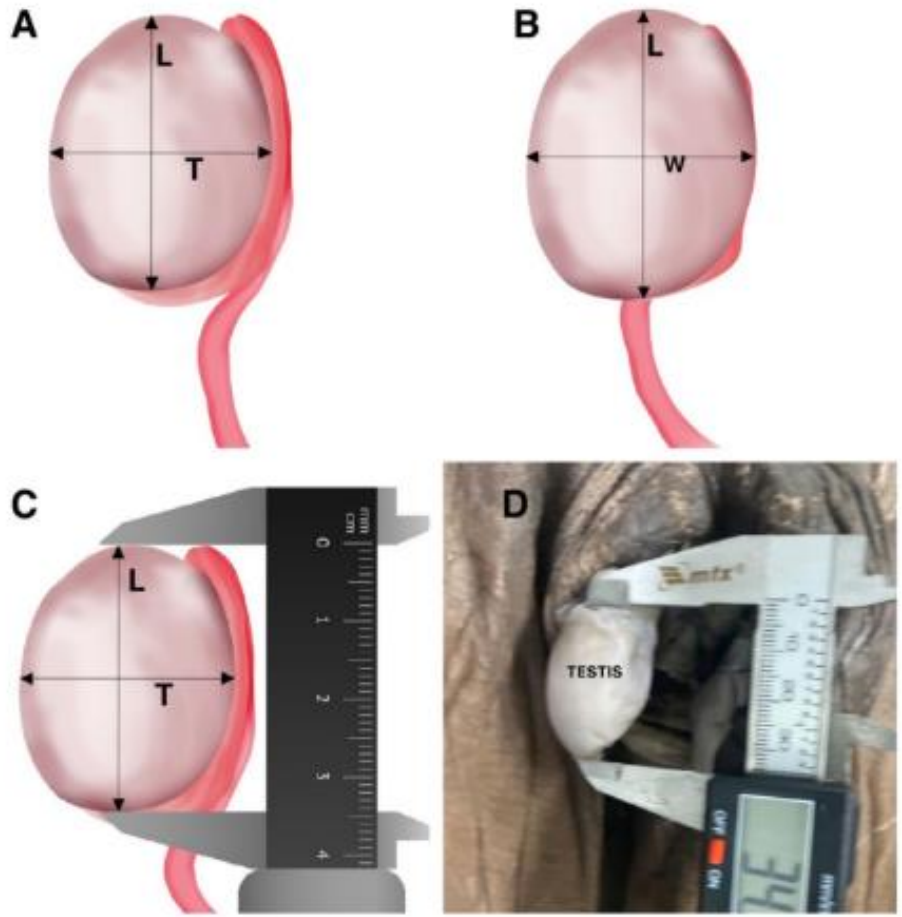

Figure 1. The figure shows a schematic drawing with the types of possible dispositions of the para-testicular apppendix found during the testicular dissections in our sample: (**A**) absence of testicular and epididymis appendix, (**B**) presence of testicular appendix (TA), (**C**) presence of epididymal appendix (EA) and (**D**) presence of testicular and epididymis appendix; T-Testis and E-Epididymis.

A medical calculator to determine testicular volumes matching ultrasound values from the width of the testis obtained in the scrotum with a centimeter ruler

Juan F. Sotos[1*] and Naomi J. Tokar[2]

Abstract

The determination of the testicular volume is of considerable importance to assess the onset, progression and disorders of puberty, abnormal testicular development, and a number of other conditions; and in adults, assessment of fertility. A number of clinical methods have been used for the measurement of testicular volumes in the scrotum: a centimeter ruler, sliding calipers, and orchidometers. All the clinical methods calculate the volumes by the ellipsoid equation, grossly overestimate ultrasound (US) volumes by 70 to 80% for adults, to 150 to 250% for prepubertal subjects, mainly because the inclusion of the scrotal skin and epididymis and may not be accurate of reproducible. Ultrasound measurements have a high degree of accuracy and reproducibility and are the standard for quantitation of testicular volume. Formulas, equivalent to the ellipsoid equations used, were developed to match ultrasound volumes, with corrections of the width and length of the testis obtained in the scrotum, to avoid the inclusion of the scrotal skin (ss) and epididymis.

A calculator was developed, requiring only the identification of ① the width of the testis in cm obtained in the scrotum with a ruler (without corrections) (i.e. 0.9, 1.5, 2.0, 2.4 cm etc.) and ② the stage of genital development. The calculator will subtract the scrotal skin for the stage of genital development, from the measurement of the width provided, apply the formula and identify the testicular volume of the subject that matches the US volume. The calculator will also provide, in a Table form, the values for the different stages of genital development.

Benefit: The information provided by the calculator will solve the problem of overestimation by the orchidometers and the external measurements, problems with the reference of values to age, and Tanner stages, would permit assessment of the beginning and progression of puberty, of micro and macroorchidism, and other conditions mentioned.

Keywords: Testicular volumes, Genital development in males, Genital stages, Orchidometers, Medical calculator

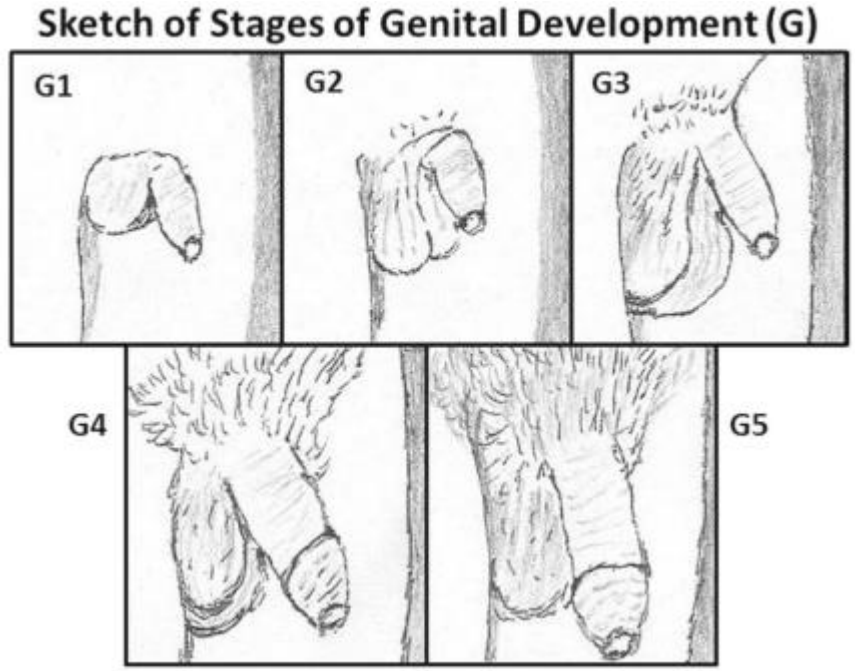

Sketch: The main characteristics of the stages of genital development (testis, scrotum and penis), independent of pubic hair development, were well defined by Tanner: G1. Prepubertal or preadolescent; the testes and the scrotum are small and penis is as in early childhood. G2. The testes and the scrotum have enlarged and there is some reddening of the scrotal skin. The penis is still as in early childhood. G3. Growth of the penis in both length and breadth and further growth of testes and the scrotum. G4. The penis has further enlarged in length and breadth with development of the glans. The testes and scrotum are further enlarged. G5. Genitalia are adult in size and shape.

Calculator for Testicular Volume

Enter the width of the testis in cm: (enter one decimal, 0 to 9)	2.2
Enter the genital stage in number: 1 to 5 (If Adult, enter A)	4
Volume of testis in ml: (equivalent to US: W x H x L x 0.71)	7.15

Testicular Volumes – $(W\text{-}ss)^3$ X 0.88 by Genital Stages

Equivalent to Ultrasound W x H x L x 0.71

Stage	Age Years range	# of Testes	Volume (ml)		
			Median	Quartiles - 25-75%	Range Observed
Stage 1-a*	3.4 to 6.5	24	0.71	0.50 to 0.71	0.50 to 0.71
1-b*	7.2 to 8.7	24	0.71	0.71 to 0.77	0.60 to 0.96
1-c*	8.9 to 13.2	32	0.96	0.71 to 1.27	0.60 to 1.27
Stage 1 All	3.4 to 13.2	80	0.71	0.71 to 0.96	0.50 to 1.27
Stage 2	10.0 to 15.0	34	3.62	2.68 to 4.00	2.16 to 6.52
Stage 3	11.4 to 15.0	22	6.42	5.48 to 6.42	4.64 to 7.47
Stage 4	11.7 to 16.9	44	10.85	8.27 to 12.32	6.13 to 12.32
Stage 5	13.0 to 17.5	38	17.32	15.47 to 17.32	10.71 to 21.46
Adult	15.8 to 34.0	100	17.13	15.29 to 21.24	10.57 to 21.24

*Stage 1a, b, c: The only criterion for separation is age (Enter the number 1 only in the Genital Stage box). For testicular volumes calculated by W x H x L x 0.52, divide values reported by 1.365 (0.71/0.52 = 1.365).

ScientificScholar®
Knowledge is power
Publisher of Scientific Journals

www.americanjs.com

American Journal of Sonography

Original Article

Sonographic Features of Chronic Kidney Disease in Agricultural Community in Sri Lanka

Muditha S. Bandara[1], Buddika Gurunayaka[2], Gamage Pemanatha Lakraj[3], Aruna Pallewatte[4], Sisira Siribaddana[5], Janaka Wansapura[6,7]

[1]Department of Physics, University of Colombo, Colombo, [2]Department of Radiology, Anuradhapura Teaching Hospital, Anuradhapura, [3]Department of Statistic, University of Colombo, Colombo, [4]Department of Neuroradiology, National Hospital of Sri Lanka, Colombo, [5]Department of Medicine, Rajarata University of Sri Lanka, Anuradhapura, [6]Department of Physics, University of Colombo, Colombo, Sri Lanka, [7]Advanced Imaging Research Center, University of Texas Southwestern, Texas, USA.

***Corresponding author:**
Janaka Wansapura,
Advanced Imaging Research Center, University of Texas Southwestern, Texas, USA.

janaka.wansapura@utsouthwestern.edu

Received : 03 December 2019
Accepted : 02 February 2021
Published : 17 March 2021

DOI
10.25259/AJS_14_2019

Quick Response Code:

ABSTRACT

Objectives: The aim of this study was to use ultrasound-based kidney morphological features to classify chronic kidney disease (CKD) in an agricultural community in Sri Lanka where there is a high prevalence of CKD with unknown etiology.

Materials and Methods: A cohort of CKD patients ($n = 50$) and healthy subjects ($n = 26$) underwent B-mode renal ultrasound. CKD patients were further categorized as those clinically diagnosed with diabetes mellitus, hypertension, and other known causes ($n = 30$) and those of unknown etiology ($n = 20$). Following kidney morphological features were calculated: Length (LEN), width (WDTH), cortical thickness, volume (VOL), and shape index.

Results: CKD kidneys of both groups were significantly smaller than the healthy kidneys ($P < 0.001$). Based on a random forest procedure, the top three influential features that distinguished CKD kidneys from healthy kidneys were: VOL normalized to waist circumference (CKD = 0.6 ± 0.2 cm^2, healthy = 0.9 ± 0.2 cm^2), VOL normalized to body surface area (CKD = 36 ± 9 cm^3/m^2, healthy = 52 ± 13 cm^3/m^2), and WDTH (CKD = 3.6 ± 0.5 cm, healthy = 4.3 ± 0.6 cm). Patients with CKD of unknown etiology had higher kidney LEN and VOL normalized to height (HGHT) (LEN/HGHT = 0.58 ± 0.05 cm/m, VOL/HGHT = 0.40 ± 0.09 cm^3/m, $P < 0.05$) compared to those of the known etiology group (LEN/HGHT = 0.51 ± 0.09 cm/m, VOL/HGHT = 0.30 ± 0.10 cm^3/m).

Conclusion: The study shows that ultrasound-based kidney volume can distinguish healthy versus diseased kidneys as well as CKD of known versus unknown etiology. Normalizing for height is required when comparing diseased groups.

Keywords: Chronic kidney disease, Kidney volume, Ultrasound

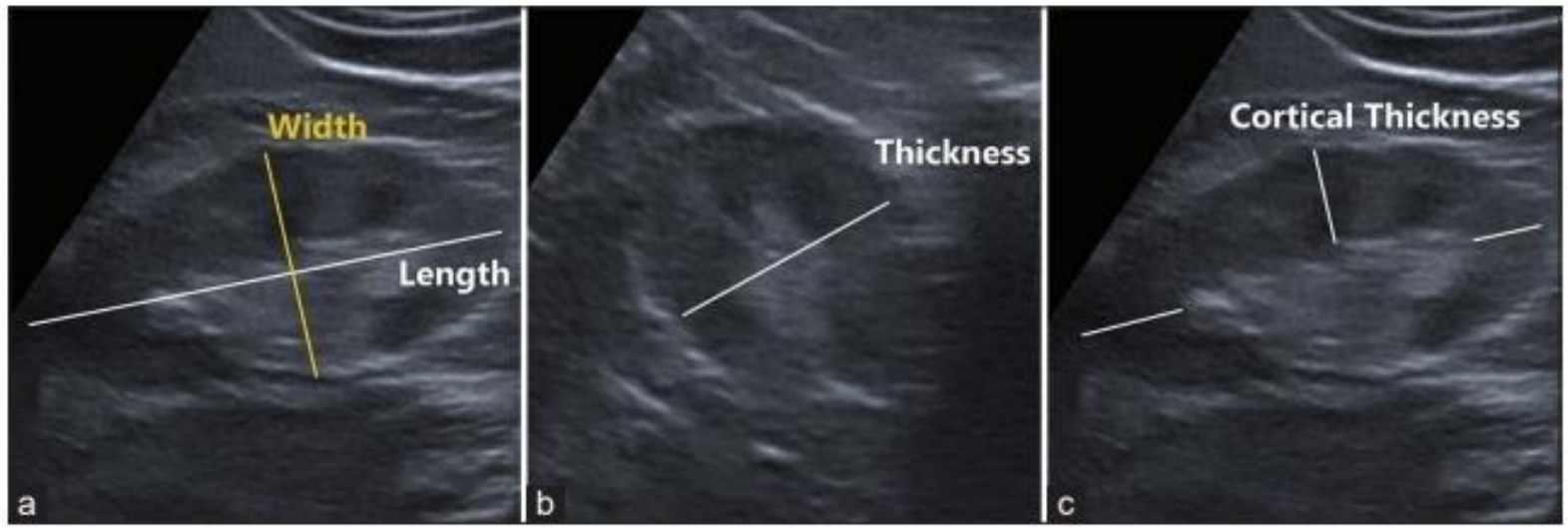

Figure 1: A 60-year-old male patient with chronic kidney disease. (a) Renal ultrasound image indicates the maximum longitudinal length (white) and maximum transverse width (yellow) measured in the coronal plane, (b) maximum thickness (THK) measured in the transverse plane, (c) cortical THK measurements in the ultrasound image from the outer border of the kidney cortex to the outer border of the medulla.

Med Ultrason 2026, Vol. 28, no. 2, 162-171
DOI: 10.11152/mu-4550

Flexor digitorum profundus evaluation in normal muscle mass subjects and presarcopenic patients – a sonoelastographic cross-sectional study

Roxana-Ioana Guțiu[1,2], Ana-Diana Bilous[2], Iulia Cozma[2], Oana Șerban[1,2], Maria Bădărînză[1,2], Daniela Fodor[1,2]

[1]"Iuliu Hațieganu" University of Medicine and Pharmacy, [2]2nd Internal Medicine Department, Cluj-Napoca, Romania

Abstract

Aim: Presarcopenia represents the earliest stage of sarcopenia. While muscle ultrasound (US) and shear wave elastography (SWE) offer promise as a non-invasive tool, its role in detecting early muscle loss remains underexplored, especially in the upper limb. Therefore, the aim of this study was to characterize the flexor digitorum profundus (FDP) muscle in older adults with presarcopenia versus normal muscle mass, and to assess the diagnostic potential of grayscale echogenicity and SWE. **Material and methods:** This cross-sectional study included 50 age- and sex-matched participants classified as presarcopenic (n=25) or normal muscle mass (n=25) based on dual-energy x-ray absorptiometry (DXA)-derived appendicular skeletal muscle mass index (ASMI). All underwent clinical evaluation and ultrasound assessment of the FDP. US parameters included cross-sectional area (CSA), muscle thickness (MT), pennation angle (PA), echogenicity, and SWE in relaxation and contraction. Logistic regression and ROC analysis were applied. **Results:** Presarcopenic participants had significantly lower CSA ($p=0.001$) and higher grayscale echogenicity ($p<0.001$). MT and PA did not differ significantly. Echogenicity showed negative correlations with CSA, DXA measurements, and forearm circumference (FC). Grayscale cut-off values were proposed to differentiate visual echogenicity grades. Although SWE values were not significantly different in univariate analysis, SWE in relaxation emerged as an independent predictor in the regression model. C**onclusions:** FDP grayscale echogenicity is a strong marker of early muscle decline. SWE in relaxation independently predicted presarcopenia, supporting its role in early diagnostic frameworks. Larger studies are warranted.

Keywords: presarcopenia; ageing; flexor digitorum profundus; SWE; ultrasound

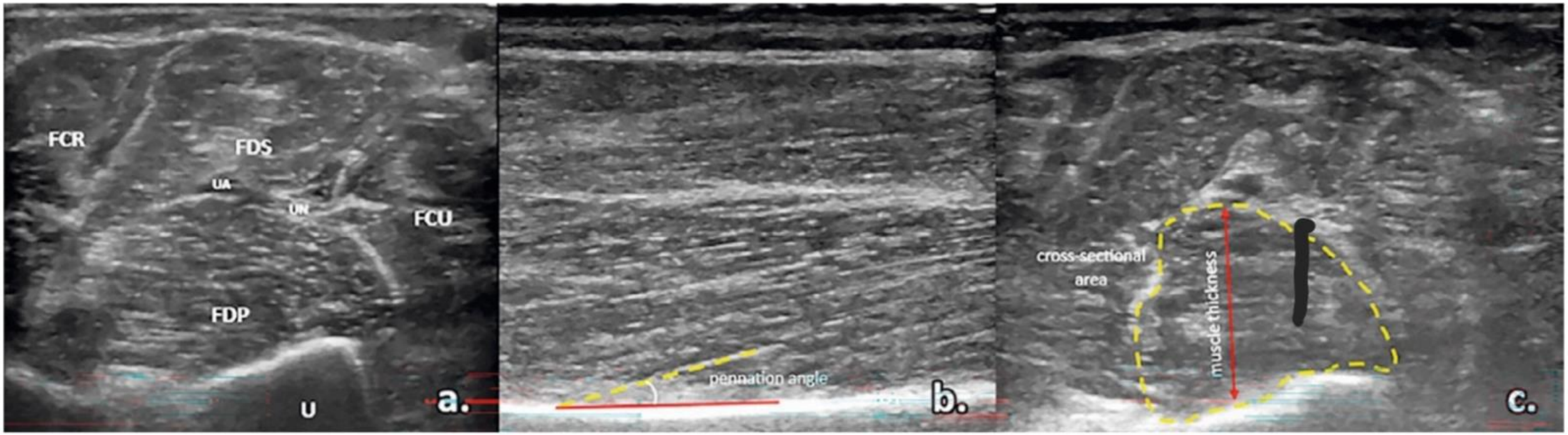

Fig 1. Grayscale ultrasound examination of the flexor digitorum profundus muscle (FDP) (a) transverse scan proximal third of the forearm; (b) longitudinal scan measurement of the pennation angle; (c) transverse scan measurement of cross-sectional area and muscle thickness. U, ulna; FCR, flexor carpi radialis muscle; FDS, flexor digitorum superficialis muscle; FCU, flexor carpi ulnaris muscle; UN, ulnar nerve; UA, ulnar artery.

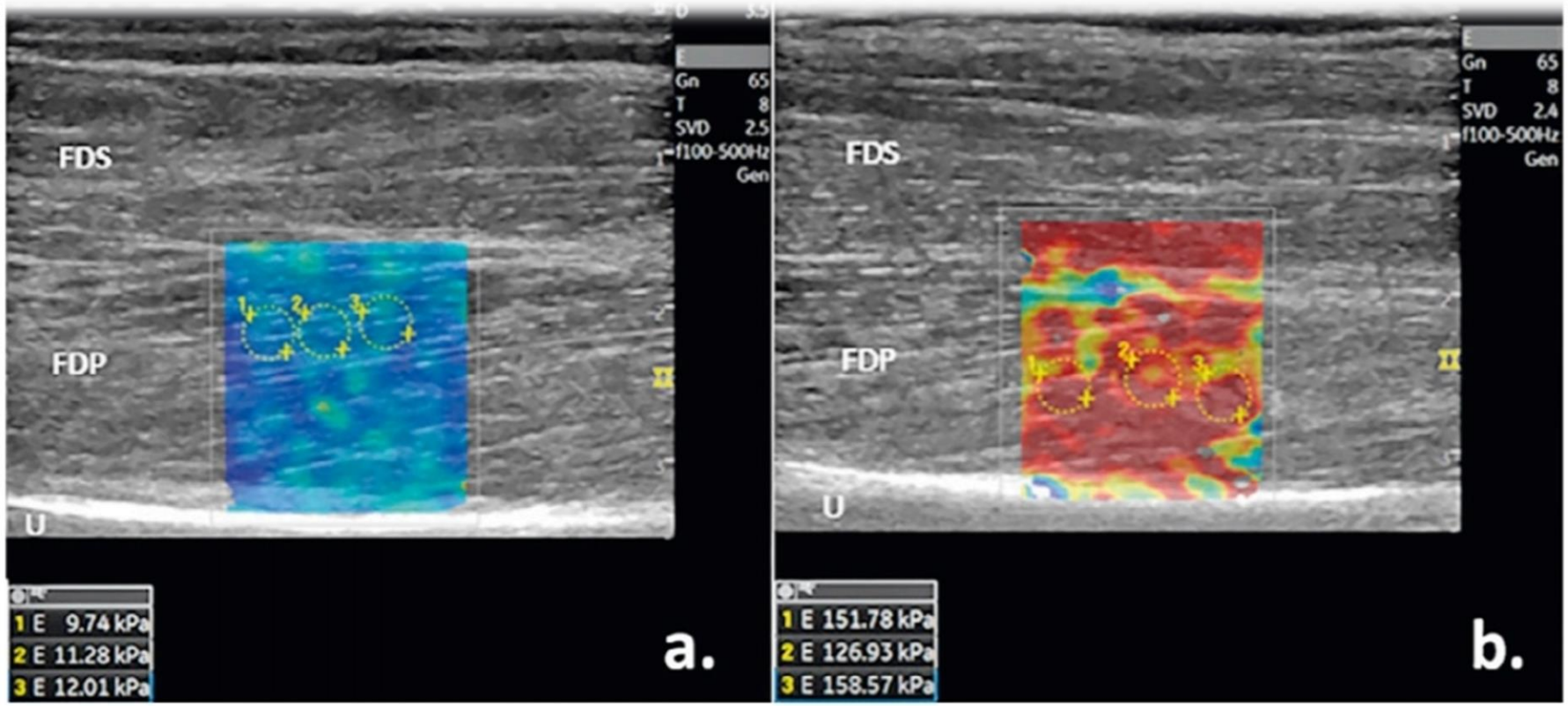

Fig 2. Longitudinal SWE of the FDP in the (a) relaxed and (b) contracted state: U, ulna; FDP, flexor digitorum profundus muscle; FDS, flexor digitorum superficialis muscle.

Cấp độ Heckmatt	Đặc điểm hình ảnh siêu âm	Ý nghĩa chất lượng cơ
Độ 1 (Bình thường)	Cơ tối (kém hồi âm), dải màng cơ rõ, vỏ xương phía sau sắc nét.	Chất lượng cơ tốt, không thâm nhiễm mỡ.
Độ 2 (Mức độ nhẹ)	Độ hồi âm của cơ tăng nhẹ, vỏ xương phía sau vẫn thấy rõ.	Thâm nhiễm mỡ nhẹ.
Độ 3 (Mức độ vừa)	Cơ sáng rõ (tăng hồi âm), vỏ xương bị mờ bớt do bị cản âm.	Thâm nhiễm mỡ và xơ hóa trung bình.
Độ 4 (Mức độ nặng)	Cơ sáng trắng hoàn toàn, **mất hoàn toàn** hình ảnh vỏ xương phía sau.	Thâm nhiễm mỡ nặng, mất cấu trúc cơ nghiêm trọng.

SCIENTIFIC REPORTS

OPEN

Ultrasonographic and elastographic biometry in adult major salivary glands: a preliminary case-control report

Received: 8 October 2018
Accepted: 4 June 2019
Published online: 20 June 2019

Kai-Min Fang[1,2], Ming-Hsun Wen[2], Wan-Lun Hsu[3], Chih-Ming Chang[2], Pei-Yu Hou[4] & Li-Jen Liao[2,5,6]

Specifications about the size and stiffness of healthy salivary glands with ultrasound (US) are not available for Asian people. Using a Toshiba Apolio 500 US platform, we determined the size (including anterior-posterior median length, median paramandibular depth dimension, and cranio-caudal height) and hardness of 100 healthy submandibular and parotid glands in volunteers without a history of disease affecting the salivary glands or post-radiation, and compared the dimensions to those of 36 parotid glands and 37 submandibular glands in post-irradiated patients. The dimensions of the parotid and submandibular glands were significantly correlated with body weight. However, the dimension of the parotid glands was not significantly correlated with that of patients with prior radiation; the shear wave velocity (SWV) significantly increased (1.99 m/s versus 2.43 m/s, p-value < 0.01). The dimension of the submandibular glands was significantly correlated with prior radiation, where the SWV also significantly increased (2.32 m/s versus 2.50 m/s, p-values < 0.01). We find that US is a useful tool for assessment of the reference dimensions and hardness of major salivary glands that may be altered by irradiation.

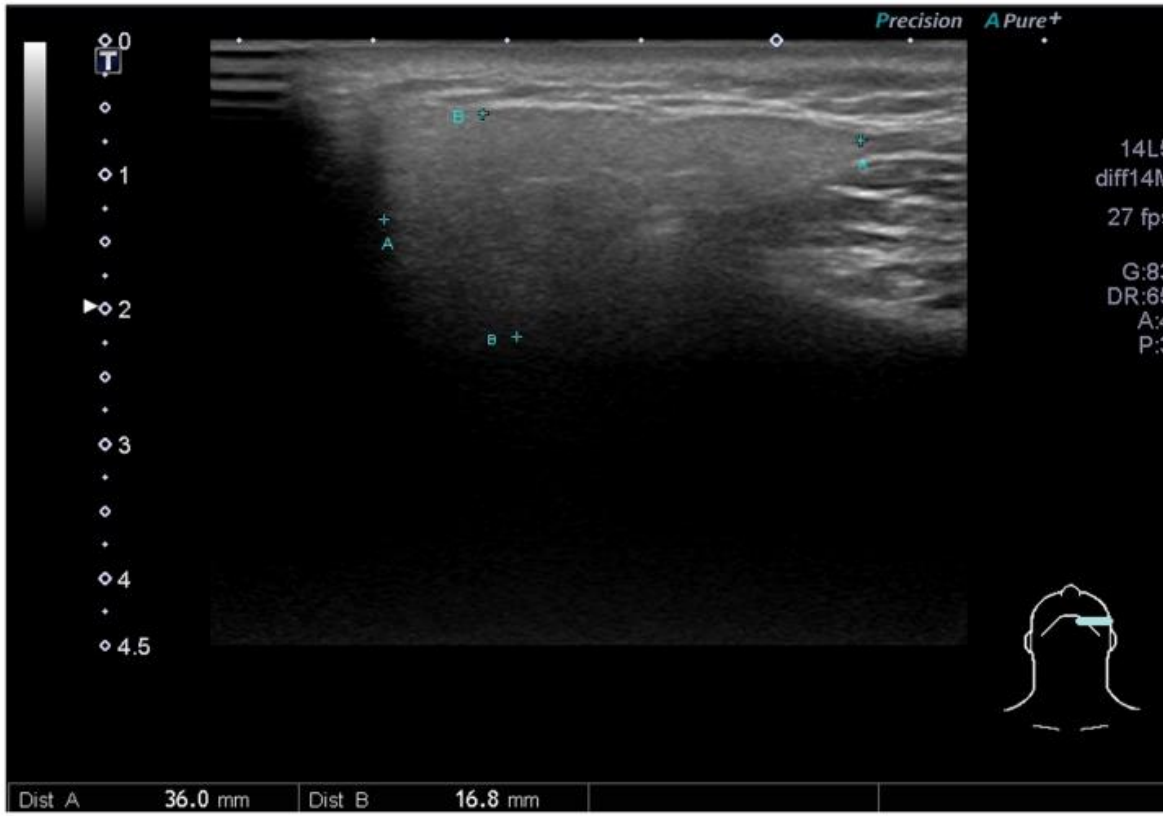

Figure 1. Dimensions of anteroposterior length (AA) and paramandibular depth (BB) of the subma gland.

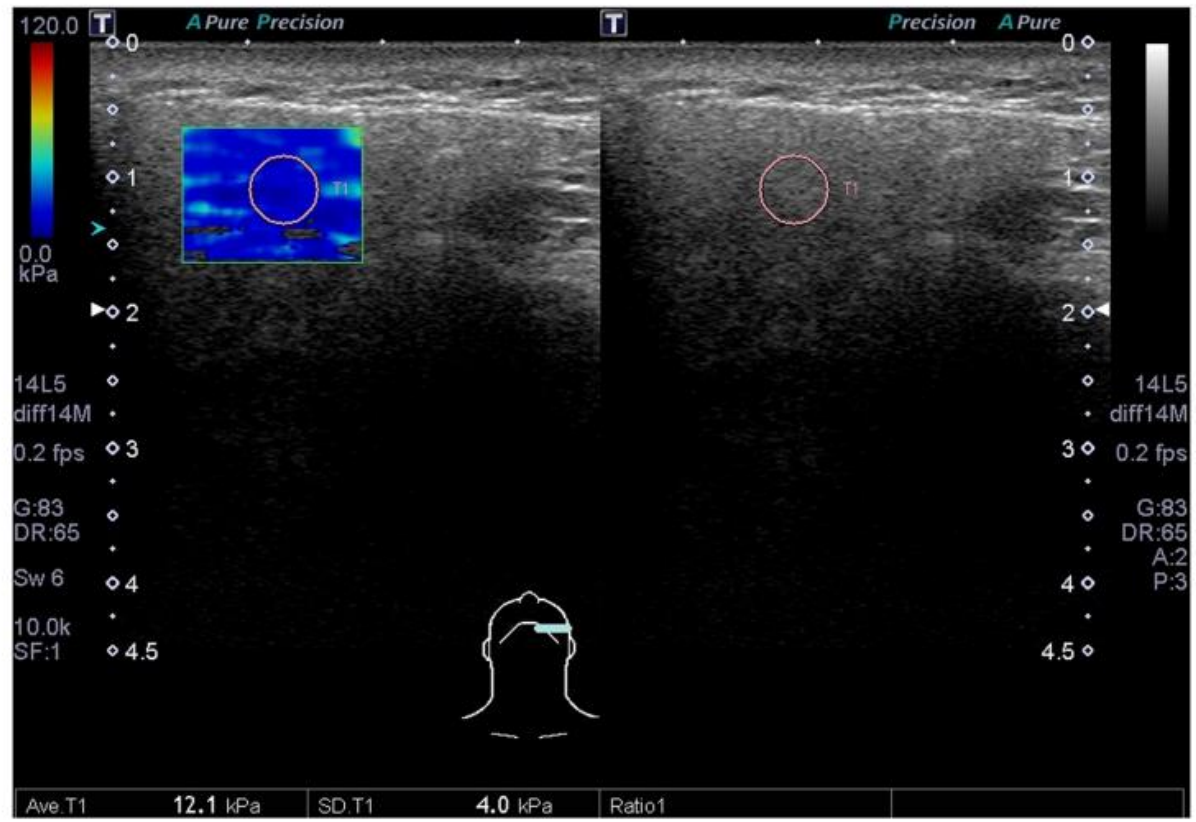

Figure 2. The SWV over the central part of the SM gland was recorded.

	Healthy Volunteers	Head and Neck Cancer Survivors	p-values
Parotid gland	N = 100	N = 36	
Anteroposterior length (mm)	36.15 (12.45)	39.35 (13.05)	0.25
Paramandibular depth (mm)	16.95 (4.00)	16.55 (4.70)	0.90
Cranio-caudal height (mm)	43.60 (10.10)	42.95 (10.00)	0.75
Central SWV(m/s)	1.99 (0.57)	2.43 (0.94)	<0.01*
Submandibular glands	N = 100	N = 37	
Anteroposterior length (mm)	34.55 (6.95)	30.40 (7.30)	<0.01*
Paramandibular depth (mm)	16.60 (3.85)	12.05 (2.70)	<0.01*
Cranio-caudal height (mm)	23.40(15.30)	22.00(13.80)	0.06
Central SWV(m/s)	2.32 (0.45)	2.50 (0.62)	0.04*

Table 2. Median and interquartile (IQR) of the dimensions and SWV for healthy volunteers compared to post RT salivary glands. *<0.05.

We find that ultrasound is a useful tool for assessment of the dimensions and hardness of major salivary glands. The dimensions and hardness of the glands are associated with body weight and previous irradiation.

This study proves that the salivary glands in an Asian population have smaller measurements than those in a European population. This study also confirms that, in this population, there is a relationship between body weight and gland size. In addition to altering the gland size, previous radiation for two or more years is shown to be correlated with smaller gland size and more fibrosis; this is confirmed with elastography.

Journal of Ultrasound > Article

Ultrasonographic evaluation of major salivary glands in patients with type 2 diabetes mellitus

Original Paper | Published: 22 April 2026

Volume 29, pages 419–426 (2026) Cite this article

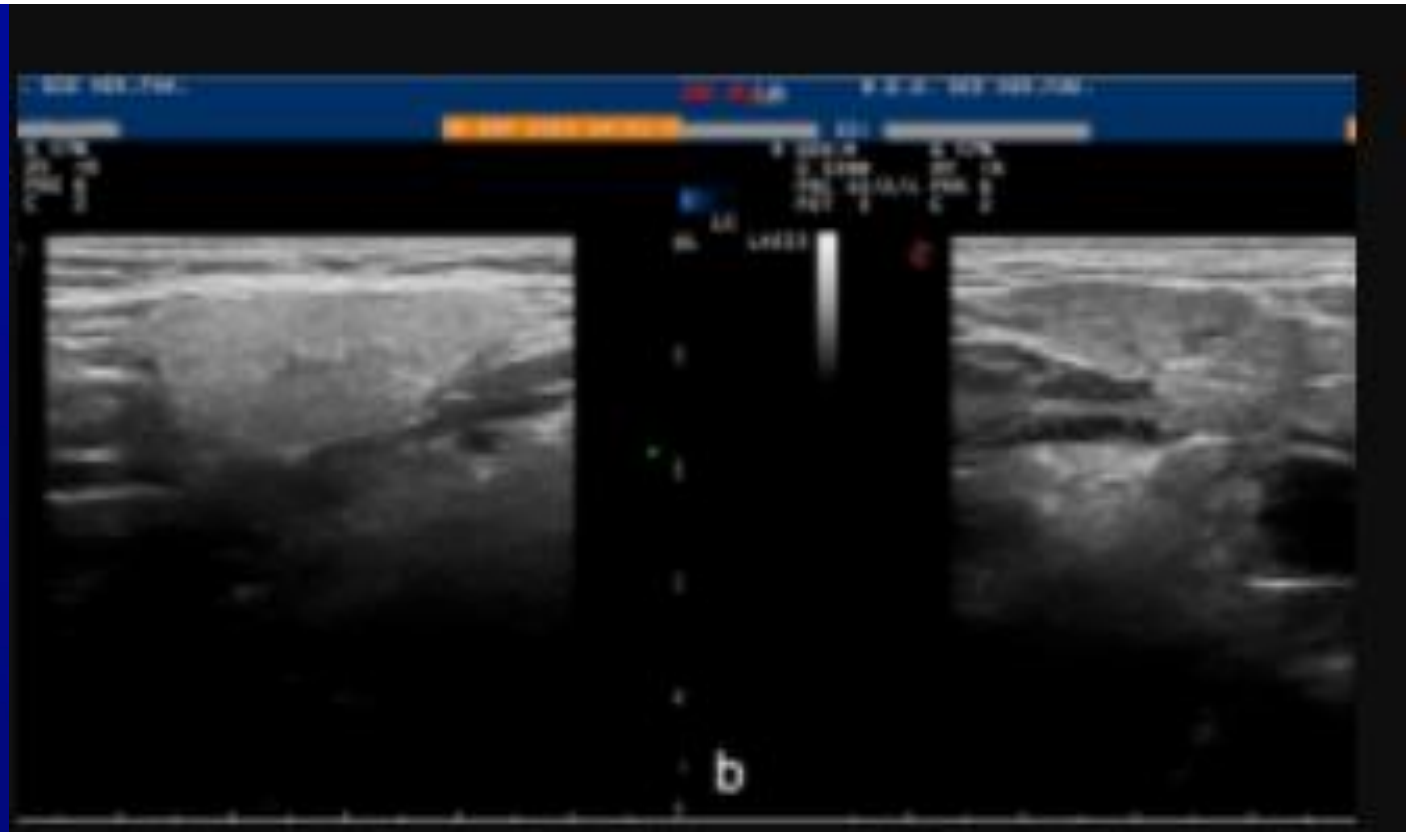

Abstract

Objective

Type 2 diabetes causes changes in the structure and functions of the major salivary glands. The aim of this study is to evaluate the dimensional measurements, echogenicity, and fractal dimension (FD) of bilateral major salivary glands in patients with type 2 diabetes mellitus (DM) on ultrasonography (US) and compare them with healthy individuals.

Methods

The study included US images of 36 patients with type 2 DM and 36 healthy individuals. The superoinferior (SI), anteroposterior (AP), and mediolateral (ML) dimensions of the major salivary glands were measured, echogenicity was classified, and FD was calculated. Dimensional measurements, FD, and echogenicity comparisons between groups were analyzed.

Results

Dimensions of SI, AP, and ML were found statistically higher in the patient group than in the control group ($p < 0.05$). In the parotid gland, the isoechoic type was significantly more common in the patient group ($p < 0.05$). Although no statistically significant relationship was observed, in the submandibular and sublingual glands, isoechoic type was more frequent in the patient group. FD values were found to be higher in the patient group compared with the control group for all glands and a statistically significant relationship was observed in the sublingual gland ($p < 0.05$).

Conclusion

Type 2 DM is a disease that changes the salivary gland structure, but to confirm these results, new studies are needed in which disease severity/HbA1c levels, drug doses and disease duration are known and can be associated with clinical data.

Breast carcinoma metastasis to the submandibular gland: Clinical, sonographic and pathological findings of a rare entity

Lamees Salman, Zainab Al Shiekh Ali, and David C Howlett View all authors and affiliations

Volume 33, Issue 1
https://doi.org/10.1177/1742271X241249066

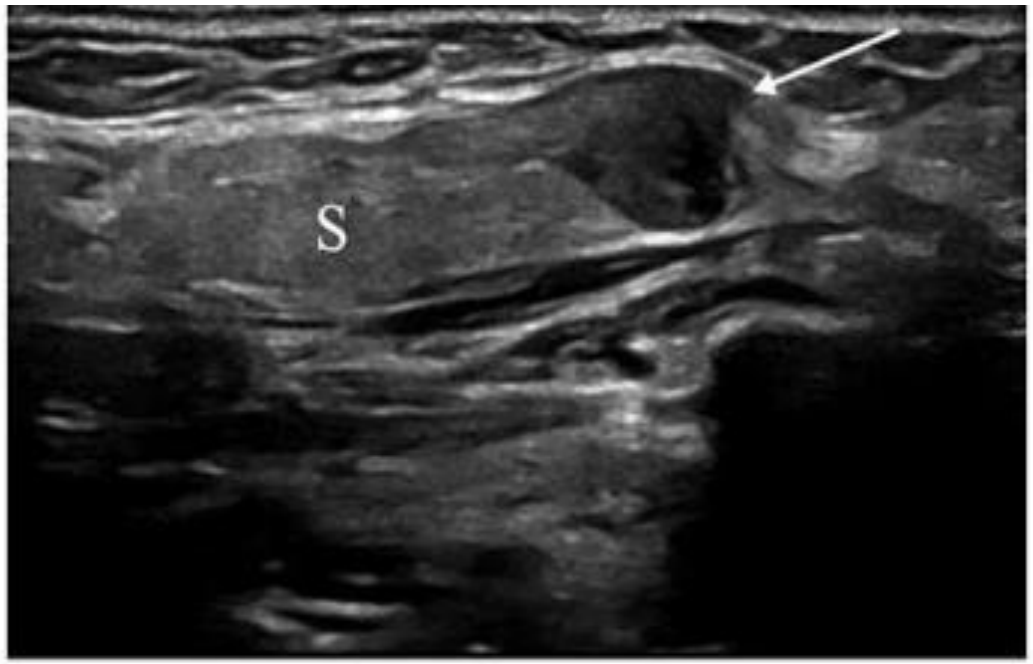

Figure 1. Grey scale sonogram of the right submandibular gland (S). The image demonstrates an ill-defined 8-mm hypoechoic mass medially within the right submandibular gland (white arrow).

Abstract

Introduction:

Metastatic disease to the submandibular gland is a rare phenomenon with limited information available on related imaging findings.

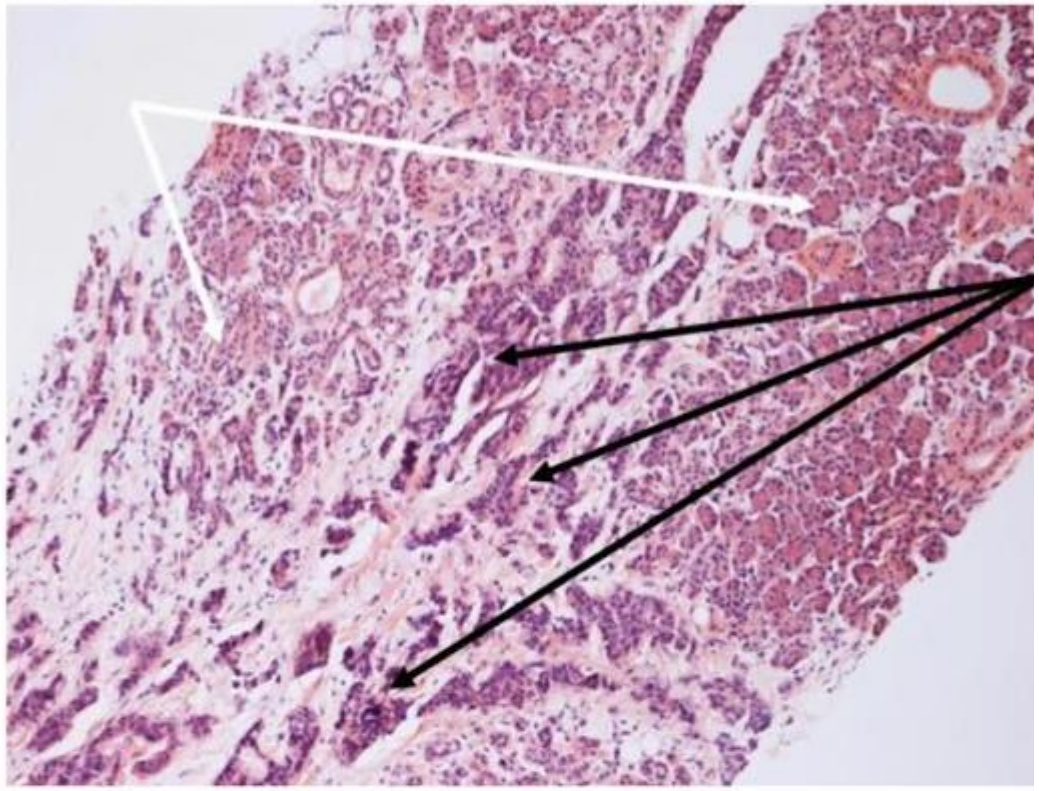

Figure 3. Haematoxylin and eosin (H&E) staining demonstrate the tumour cells (black arrows) infiltrating into the submandibular gland tissue (white arrows) in keeping with breast adenocarcinoma metastasis of the submandibular gland.

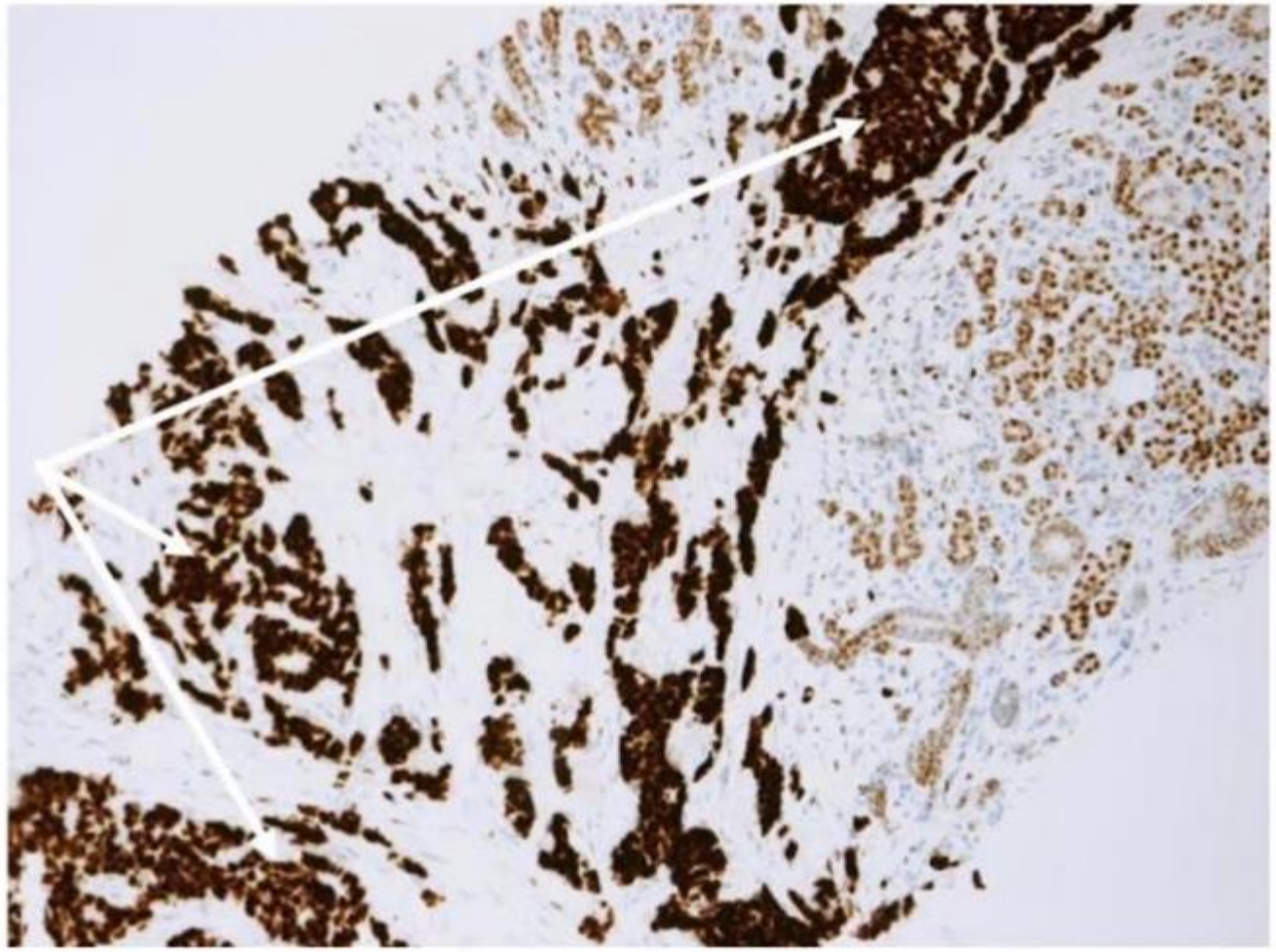

Figure 4. IHC staining of the tumour cells (white arrows) show strong nuclear positivity for GATA3.

Ultrasound
Volume 33, Issue 1, February 2025, Pages 58-65

https://doi.org/10.1177/1742271X241275136

Sage Journals

Pictorial Essay

Sarcoma or haematoma? If only it was that simple! Part 1

Catharine Berry[1] **and Mark Charnock**[2]

Introduction: Imaging appearances and clinical presentation of soft tissue sarcoma and soft tissue haematomas are similar. It is imperative that sarcoma is differentiated from benign soft tissue lesions due to the poor outcomes and high morbidity associated with sarcoma.

Topic description: Part 1 of this pictorial review will summarise the paucity of guidance in management of suspected haematomas, the clinical features and ultrasound techniques used in the assessment of soft tissue masses.

Discussion: Ultrasound is the first-line test in the investigation of soft tissue masses. With the overlapping ultrasound appearances of soft tissue sarcoma and soft tissue haematoma, thorough and methodical clinical examination and scanning technique is fundamental so that practitioners understand when to escalate cases for further investigation.

Conclusion: The clinical assessment and clinical history taking into consideration the intensity of trauma and ecchymosis must correlate with the ultrasound appearances. This will facilitate an accurate diagnosis, timely management and improved patient outcomes.

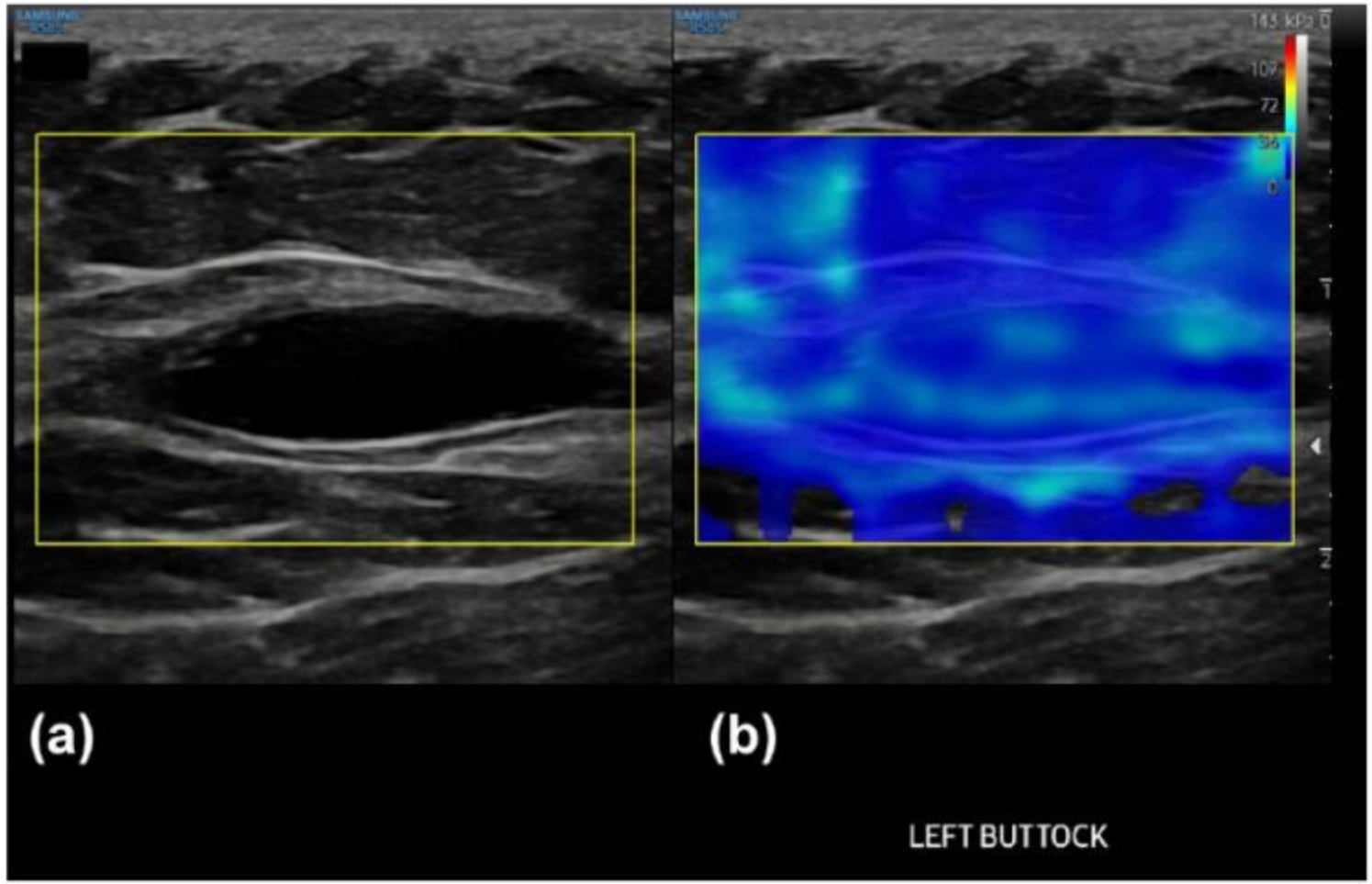

Figure 6. (a) Transverse ultrasound image of a haematoma in the subcutaneous tissues of the left buttock. (a) The B-mode image. (b) The lesion has the same stiffness as the surrounding subcutaneous tissues. The haematoma was followed up and had resolved on a subsequent ultrasound scan.

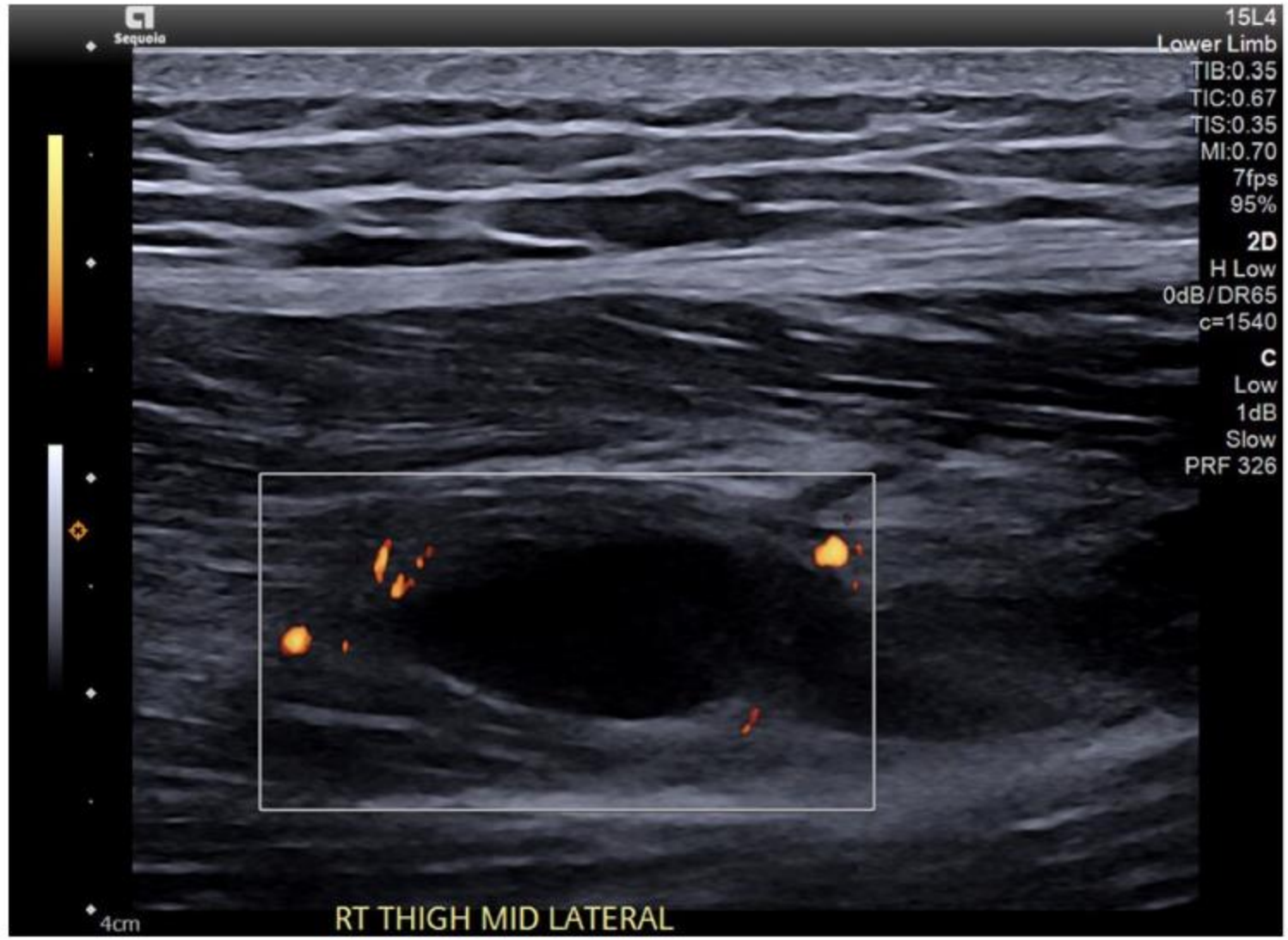

Figure 9. Transverse ultrasound image of an intramuscular haematoma in the right lateral thigh from the same patient as Figure 7. Microvascular imaging reveals no vascularity in the haematoma.